AIAA SciTech Forum
12-16 January 2026, Orlando, FL
AIAA SCITECH 2026 Forum

10.2514/6.2026-2306

Performance Testing of Small Multi-Rotor UAV Propellers

Brendan Cox* and Or D. Dantsker†
Indiana University, Bloomington, IN 47408

The increase in popularity of unmanned aerial vehicles (UAVs) has been driven by their use in civilian, education, government, and military applications. However, limited on-board energy storage, especially on multi-rotor UAV, significantly limits their flight time and ultimately usability. The propulsion system plays a critical part in the overall energy consumption of the UAV, and therefore it is necessary to determine the most optimal combination of possible propulsion system components for a given mission profile, i.e., propellers, motors, and electronic speed controllers (ESC). Hundreds of options exist for small propellers, but almost none include verified performance metrics. This paper describes the performance testing of 18 fixed-blade propellers with diameters of 40 to 102 mm (1.57 to 4.02 in) that are recommended for multi-rotor UAV applications. The propellers were tested in static conditions up to a max RPM of 18,000-38,000, depending on propeller diameter. Results are presented for the 18 propellers tested with several key observations being discussed.

Nomenclature

ESC	=	electronic speed controller	P	=	propeller power
PWM	=	pulse width modulation	Q	=	torque
RPM	=	rotations per minute	R	=	universal gas constant
UAV	=	unmanned aerial vehicle	T	=	thrust, ambient temperature
C_P	=	power coefficient	ρ	=	density of air
C_T	=	thrust coefficient	η_{static}	=	static efficiency
D	=	propeller diameter	M_{tip}	=	propeller tip Mach number
n	=	propeller rotation rate	γ	=	ratio of specific heats
p	=	ambient pressure			

I. Introduction

In recent years, there has been an uptrend in the popularity of UAVs driven by the desire to apply these aircraft to areas such as precision farming, infrastructure and environment monitoring, surveillance, surveying and mapping, search and rescue missions, weather forecasting, and more. A key design constraint among all unmanned aircraft has been energy storage, which significantly limits flight time and ultimately usability. This is especially important for multi-rotor aircraft where thrust makes up all of aircraft's lift and maneuvering force. Similarly on lighter-than-air (LTA) vehicles, significant propulsion performance is required for maneuvering due to the high vehicular drag. Therefore, the critical choice in UAV development then becomes what type of propulsion system to use.

In previous work, a mission-based propulsion system optimization tool was developed for fixed-wing unmanned aircraft[1] to select the most optimal combination of possible propulsion system components for a given mission profile, i.e., propellers, motors, and ESCs. Currently, there are hundreds of propeller and dozens of motor and ESC options in

*PhD Student, Department of Intelligent Systems Engineering, AIAA Student Member. brewcox@iu.edu
†Assistant Professor, Department of Intelligent Systems Engineering, AIAA Member. odantske@iu.edu

the radio control model market for small- to medium-sized (1-3 m wingspans) fixed-wing aircraft, yielding thousands of possible choices. Therefore, the problem became gathering component parameters with often scarce performance specifications. Recent propeller testing efforts by the authors have measured electric fixed- and folding-blade propellers from manufacturers such as APC, Master Airscrew, AeroNaut, Graupner, Kavan, etc.,[2–4] which are mostly suited to fixed-wing unmanned aircraft.

However, in examining the non-fixed wing unmanned aircraft, for example the aforementioned multi-rotor and light-than-air vehicles, there is a similar need to optimize their propulsion system for both performance and endurance requirements. Particularly, one ongoing effort that requires significant propeller data is the design of lighter-than-air vehicles for the Defend The Republic (DTR) competition.[5,6] At the DTR competition, collegiate teams strive to create the most competitive LTA vehicles with significant physical constraints in a head-to-head competition as an exploration into the research necessary for autonomous aerial vehicles.[7–19] During the competition, students aim to have their vehicles capture neutrally-buoyant goal balloons, and place them through colored, multi-shaped hoops on the opposing end of the playing field with limited sensing, actuation, and computational capabilities. The major constraints on physical designs is a maximum helium budget, and a maximum negative buoyancy of 100 grams. Thus, the lift requirement drives the need for efficient propulsion systems design and therefore appropriately-sized propeller performance data.

Previous works have measured the performance and efficiency parameters of propellers as well as other electric UAV propulsion system components. Brandt[20,21] and Uhlig[22,23] explored the performance of low-Reynolds number propellers at slow speeds and past stall. Lundstrom performed a similar test using an automotive-based testing rig.[24,25] Deters looked into the performance of micro propellers for both small/micro air vehicles,[26,27] later expanding his work to look at static performance of micro propellers for quadrotors.[28,29] Lindahl[30] tested large UAV propellers in a wind tunnel while Chaney[31] and Dantsker[32] did so using automotive based rigs. Lindahl also tested the effects of using different motors with a given propeller. Drela has done extensive work testing and modelling motors and propellers.[33–35] Green[36] and Gong[37] have modelled and tested the efficiency of ESCs. Gong has also tested a propeller-motor combination in a wind tunnel[38] as well as create an in-flight thrust measurement system.[39] The authors have previously static performance tested micro propellers for quadcopters.[29] However, a larger set of propeller data is needed to enable widespread optimization of multi-rotor and light-than-air (LTA) UAVs, such as the DTR vehicles. Through the testing and proper choice of these propellers, the efficiency of both lighter-than-air vehicles for the DTR competiton and small multi-rotor vehicles can be greatly improved, allowing for longer mission times and faster vehicles.

This paper describes the static performance testing of 18 small propellers with diameters ranging from 40 to 102 mm that are recommended for multi-rotor UAV applications. This paper first presents the experimental methodology, including the equipment, testing procedure, calibration, and data reduction. Results and discussion are then given, followed by the performance results for the 18 propellers tested. Finally, a summary and statement of future work is given.

II. Experimental Methodology

A. Equipment

Propeller tests were conducted at the Indiana University Aerospace Systems Lab using the thrust and torque balance[40] shown in Fig. 1. The propellers will be mounted to the motor so that the thrust force is pointed toward the balance. With this propeller configuration, the propwash will be directed away from the balance so that it would not interfere with the measurements. Thrust will be measured using a 2 kg (4.41 lb) load cell. The torque from the propeller will be measured using a 50 oz-in and 10 oz-in reaction torque sensor (RTS). Each propeller will be tested using an appropriately-sized brushless motor using a speed controller. To provide power to the motor, a power supply will be used. Propeller RPM will measured via a Futaba SBS-01RO Optical RPM Sensor. The ambient pressure and temperature will be measured using an BMP690 pressure and temperature sensor.

Table 1: Specifications of the Propulsion Testing Apparatus

Data acquisition system	Arduino Giga R1 WiFi, Arduino Nano ESP32
Sensors	
Thrust Cell	Phidgets S-Type Load Cell - 2kg
Torque Cell	Transducer Techniques 50 oz-in and 10 oz-in RTS reaction torque sensors
Wheatstone Bridge	Phidget Bridge 4-Input
RPM	Futaba SBS-01RO Optical RPM Sensor
Current	DFRobot Isolated AC/DC 50A Current Sensor
Voltage	Analog Pin (ADC) on Arduino using Voltage Divider Circuit
Baro/Pressure/Temperature	Adafruit BMP390
Drivers	
Motor	iFlight XING2 1404 4600KV brushless motor
Speed Controller	Castle Phoenix Edge Lite 50
Power Supply	BK Precision
PWM Generator	Digital Pin on Arduino

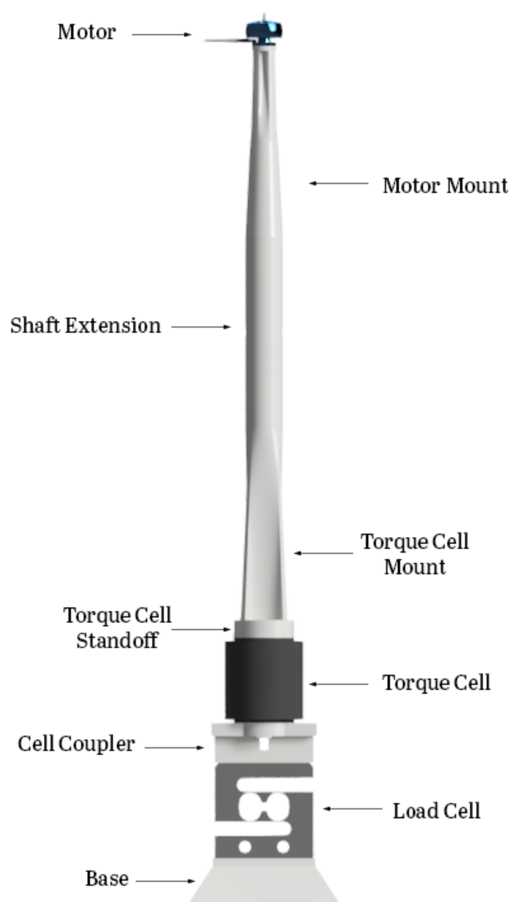

Figure 1: Propeller thrust and torque balance.

B. Testing Procedure

As a static performance test, the thrust and torque will be measured over a range of RPMs. The combination of a 2 kg load cell, 50 oz-in or 10 oz-in RTS, Futaba SBS-01RO Optical RPM Sensor, Arduino ADC voltage sensor, DFRobot Isolated AC/DC 50A Current Sensor, and BMP390 will be used to measure thrust, torque, RPM, voltage, current, ambient temperature, and ambient pressure. To control RPM, the Arduino Giga R1 WiFi will be used to generate a PWM signal between 1000 and 1300 μsec, which will be sent to the speed controller. Each increment will be commanded for 5 sec (with a 2 second warm-up), allowing for over 3000 torque and thrust data points to be collected for each PWM value. Specifications regarding the data acquisition system are summarized in Table 1.

C. Calibration

Since the outputs from the torque transducer and load cell are read as simple voltages, each voltage will be converted to a physical measurement through calibration curves. Thrust calibration will use precisely measured weights placed securely on top of the apparatus to simulate thrust on the load cell. By increasing and decreasing a known force on the load cell, a linear relationship between the thrust and voltage will be determined. For torque calibration, the precision weights will be hung using a low friction pulley along a known moment arm to create a torque, and by adding and removing weights, a linear relationship between the torque and voltage will be calculated. Before each propeller test, zero load voltage offsets are calculated to account for sensor drift.

D. Data Reduction

As mentioned in Section A, the ambient pressure and temperature are measured using a pressure and temperature sensor. Air density is then calculated from the equation of state

$$p = \rho R T \tag{1}$$

where R is the universal gas constant. The standard value of 1716 $\mathrm{ft^2/s^2/{}^\circ R}$ (287.0 $\mathrm{m^2/s^2/K}$) for air was used.

Propeller power is calculated from the measured propeller torque by

$$P = 2\pi n Q \tag{2}$$

Performance of a propeller is typically given in terms of the thrust and power coefficients, defined as

$$C_T = \frac{T}{\rho n^2 D^4} \tag{3}$$

$$C_P = \frac{P}{\rho n^3 D^5} \tag{4}$$

where nD can be considered the reference velocity and D^2 can be considered the reference area.

The static efficiency of the propeller is used to determine performance, defined as the ratio of thrust produced to the mechanical power required:

$$\eta_{static} = \frac{T}{P} \tag{5}$$

where T is the measured thrust and P is the mechanical power calculated in Equation 2.

The compressibility effects on the propeller are characterized by the tip Mach number, defined as the ratio of the blade tip speed to the local speed of sound

$$M_{tip} = \frac{\pi n D}{a} \tag{6}$$

where the local speed of sound, a, is calculated assuming an ideal gas behavior

$$a = \sqrt{\gamma R T} \tag{7}$$

with γ representing the ratio of specific heats, taken as 1.4 for air.

III. Results and Discussion

A total of 18 propellers with diameters ranging from 40 to 102 millimeters (1.57 to 4.02 in) were tested for this paper. Table 2 lists each propeller with their specific diameters and max RPM, thrust, torque, and tip mach number measured. Both the left and right versions of each propeller were tested to check for possible differences in performance.

In most cases, the left and right versions of each propeller performed (expectedly) very similarly to each other. The only minor exceptions to this occurred in the thrust coefficient graphs at low RPM ranges, as seen in Figures 6a, 8a, 12a, and 24a. One possible reason for this lies in the 2 kg load cell used to measure thrust. This load cell is rated to measure forces up to around 19.6 Newtons of force, while the largest thrust produced by a propeller in these tests was only 1.56 Newtons. The closer forces get to the lower end of a load cell's range, the less precise those measurements become. The relatively small thrust values at the beginning of these tests may explain the discrepancies found between the thrust coefficients of the left and right propeller versions at low RPM values.

The most fair comparisons between these propellers occur between those of equal diameter and equal blade count. Under those criteria, there are 5 comparison groups that can be created using the 18 propellers tested for this paper: 1.6 in 3 blade, 2 in 2 blade, 2.5 in 3 blade, 3 in 3 blade, and 4 in 2 blade propellers. Three different graphs are used to compare their performance: thrust vs rpm, power vs rpm, and efficiency vs thrust.

The 1.6 in 3 blade propeller group show predictable trends between the Gemfan 1608 and Gemfan 1611. As seen in Figures 38a and 38b, the 1611 produces more thrust and power as compared to the 1608 at each RPM value. Due to the steeper pitch of the 1611, this is to be expected. Fig. 39 shows that the two propellers are near identical in efficiency for most of the curve, but the 1608 does boast noticeably higher efficiency at lower thrust values. Moving onto the 2 in 2 blade propeller group, Figures 40a and 40b follow a similar trend as the 1.6 in propellers, with the steeper pitch Gemfan Hurricane 2015 beating out the Gemfan Hurricane 2008 in both thrust and power vs RPM. Fig. 41 once again has the lower pitch propeller beating out the higher pitch in lower thrust values, but the 2015 takes a significant lead in efficiency at higher thrust values. Due to a larger difference in pitch values in this comparison than the last, differences in efficiency are more apparent. The next category, 2.5 in 3 blade, shows the same expected relationship between steeper pitch and higher thrust and power vs PWM, as shown in Figures 42a and 42b. The difference in efficiency, however, is rather one-sided in this comparison. Fig. 43 shows the Gemfan Hurricane 2520 beating out the Gemfan Hurricane 2512 across the entire spectrum of thrust values. Next is the 3 in 3 blade category, which compares three different propellers: the Gemfan Hurricane 3016, Gemfan 3020, and Gemfan WinDancer 3028. Figures 44a and 44b once more show that higher pitch leads to more thrust and power per RPM. Interestingly, Fig. 45 shows the highest pitch 3028 boasting the most efficiency at early thrust values, with the medium pitch 3020 performing the worst. These values seem to even out almost entirely between the three propellers as thrsut values increase, however. Finally, the 4 in 2 blade group show noticeably smaller differences, but the same trend for the thrust and power vs RPM comparisons as seen in Figures 46a and 46b. This time, however, Fig. 47 shows the smaller pitch Gemfan Hurricane 4024 beating out the Nazgul 4030 in efficiency in the lower thrust ranges, with differences decreasing as thrust increases.

Propeller	Diameter (mm)	Max RPM	Max Thrust (N)	Max Torque (Nm)	Tip Mach Number
Gemfan 1610 (2 blade)	40	37,975	0.22	0.0013	0.23
Gemfan 1608 (3 blade)	40	36,151	0.26	0.0018	0.22
Gemfan 1611 (3 blade)	40	35,221	0.27	0.0019	0.21
Gemfan 45mm (3 blade)	45	33,451	0.36	0.0023	0.23
Gemfan 2020 (4 blade)	50	26,340	0.52	0.0040	0.20
Gemfan Hurricane 2008 (2 blade)	51	37,358	0.29	0.0015	0.29
Gemfan Hurricane 2015 (2 blade)	51	33,240	0.40	0.0023	0.26
Gemfan Hurricane 2009 (3 blade)	52	35,331	0.34	0.0019	0.28
Gemfan Hurricane 2520 (3 blade)	64	28,435	1.03	0.0077	0.28
Gemfan Hurricane 2512 (3 blade)	65	35,573	0.88	0.0054	0.35
Gemfan Hurricane 3018 (2 blade)	76	28,927	1.15	0.0076	0.33
BetaFPV T3X3X3 (3 blade)	76	19,964	1.33	0.0121	0.23
Gemfan 3020 (3 blade)	76	26,043	1.27	0.0089	0.30
Gemfan Hurricane 3016 (3 blade)	76	26,589	1.28	0.0087	0.31
Gemfan WinDancer 3028 (3 blade)	77	24,608	1.27	0.0096	0.29
Gemfan 353D (3 blade)	89	18,940	1.07	0.0125	0.26
Nazgul T4030 (2 blade)	101	18,009	1.55	0.0136	0.28
Gemfan Hurricane 4024 (2 blade)	102	18,591	1.56	0.0131	0.29

Table 2: Table of all propellers tested for this paper

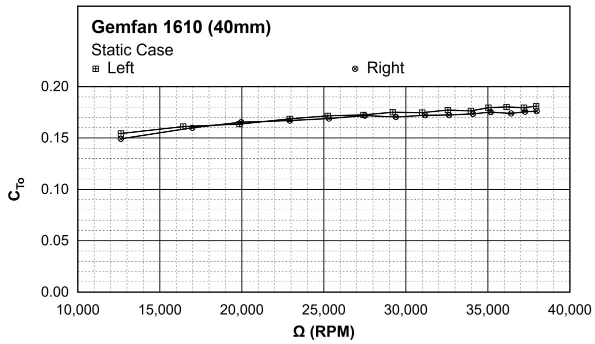

(a)

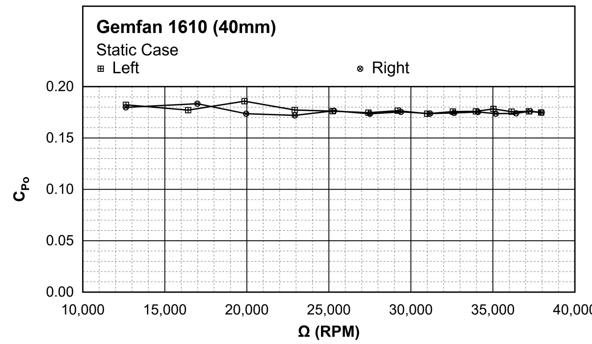

(b)

Figure 2: Comparison of static performance of the left and right versions of the Gemfan 1610 propeller: (a) thrust coefficient and (b) power coefficient

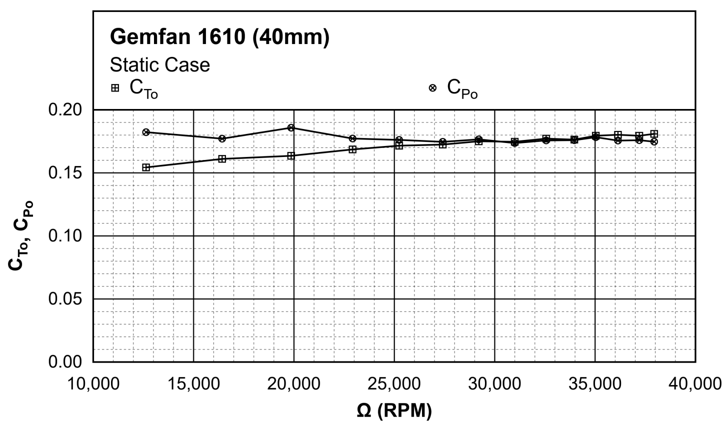

Figure 3: Combined plot of thrust coefficient and power coefficient of the left Gemfan 1610 propeller

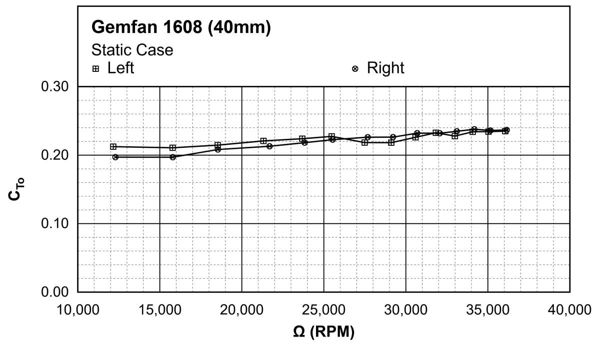

(a)

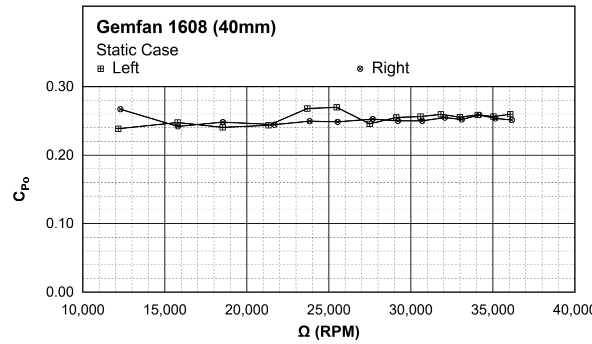

(b)

Figure 4: Comparison of static performance of the left and right versions of the Gemfan 1608 propeller: (a) thrust coefficient and (b) power coefficient

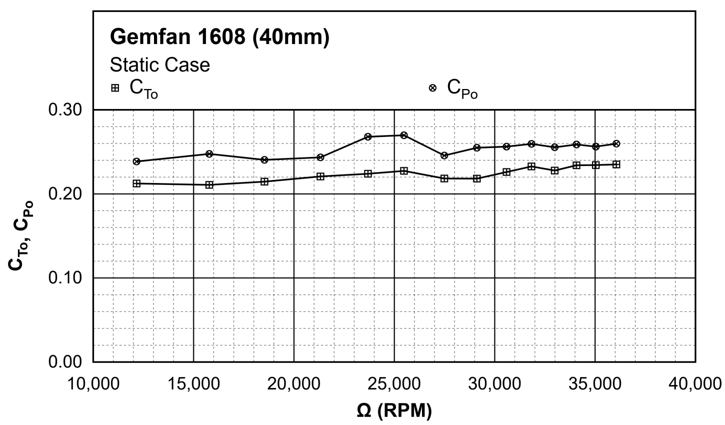

Figure 5: Combined plot of thrust coefficient and power coefficient of the left Gemfan 1608 propeller

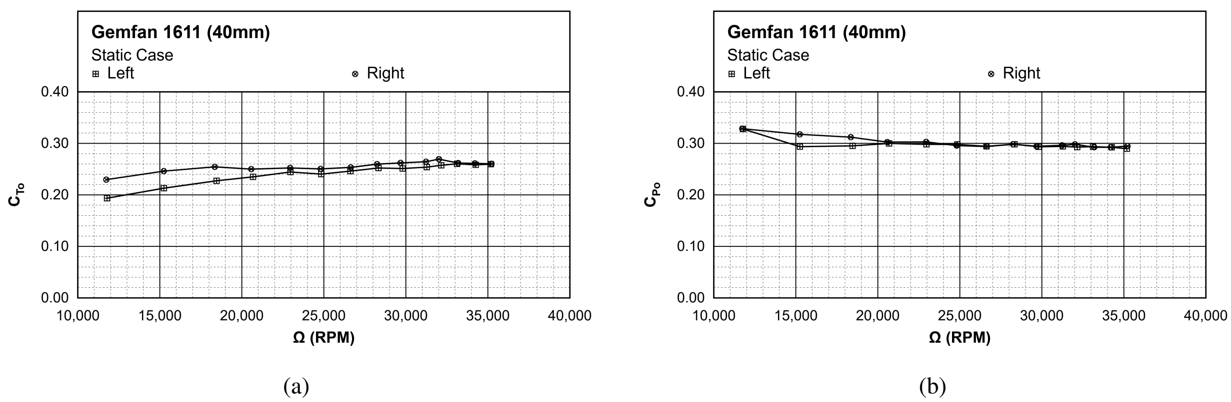

Figure 6: Comparison of static performance of the left and right versions of the Gemfan 1611 propeller: (a) thrust coefficient and (b) power coefficient

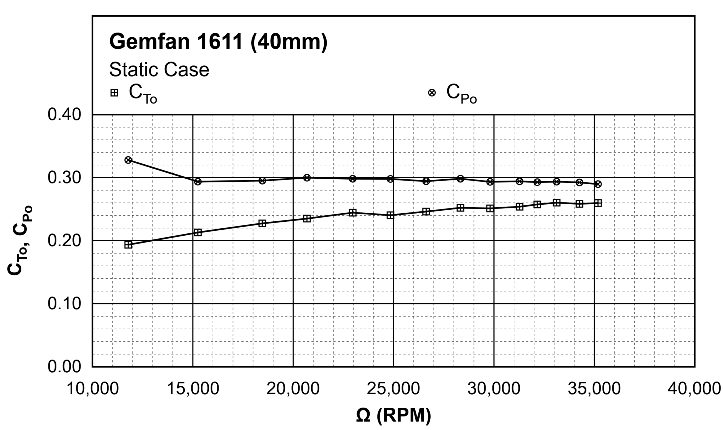

Figure 7: Combined plot of thrust coefficient and power coefficient of the left Gemfan 1611 propeller

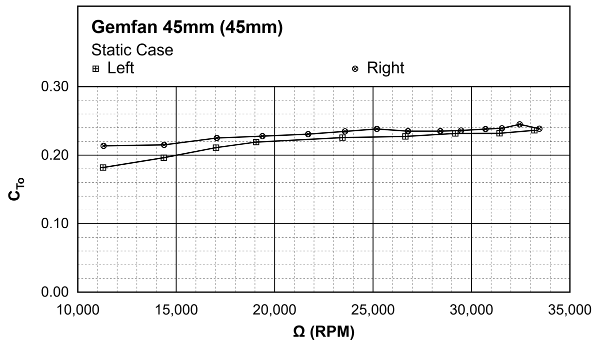

(a)

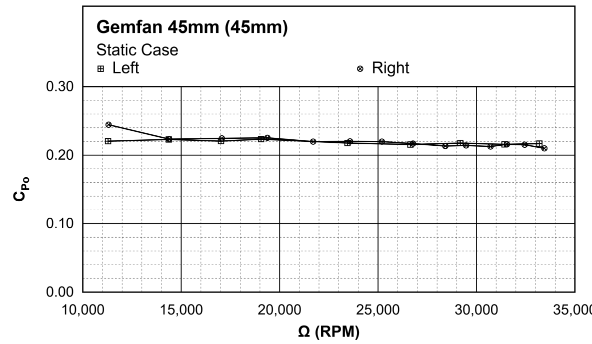

(b)

Figure 8: Comparison of static performance of the left and right versions of the Gemfan 45mm propeller: (a) thrust coefficient and (b) power coefficient

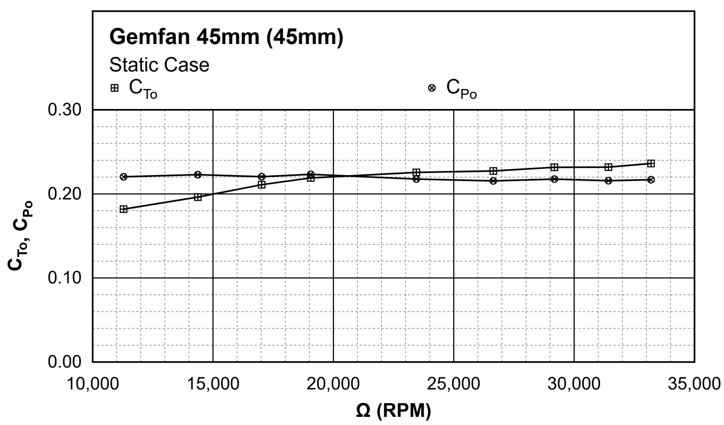

Figure 9: Combined plot of thrust coefficient and power coefficient of the left Gemfan 45mm propeller

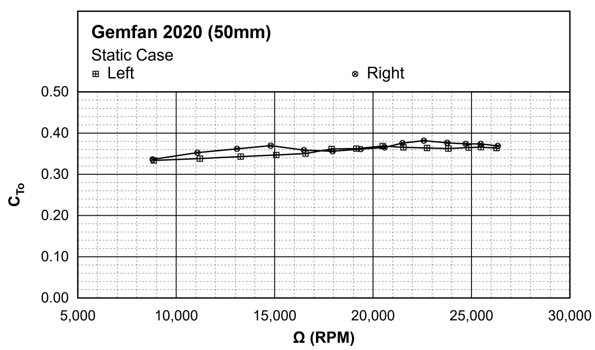

(a)

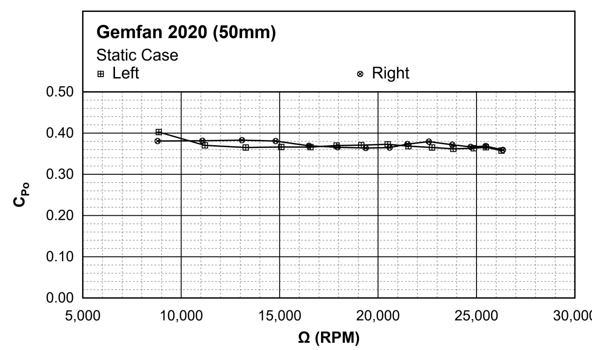

(b)

Figure 10: Comparison of static performance of the left and right versions of the Gemfan 2020 propeller: (a) thrust coefficient and (b) power coefficient

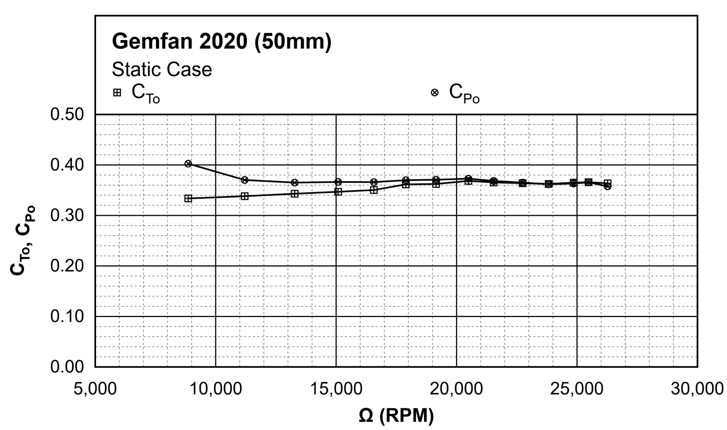

Figure 11: Combined plot of thrust coefficient and power coefficient of the left Gemfan 2020 propeller

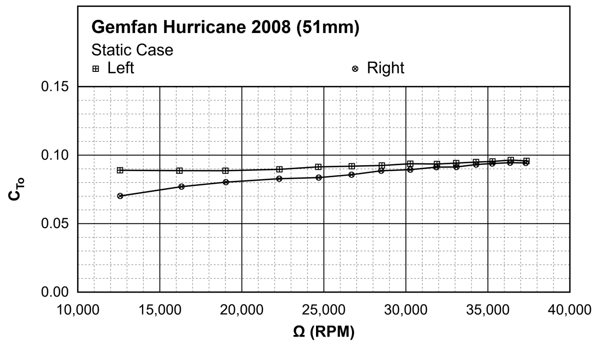

(a)

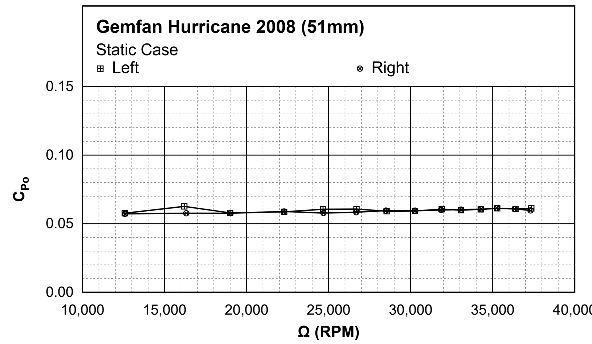

(b)

Figure 12: Comparison of static performance of the left and right versions of the Gemfan Hurricane 2008 propeller: (a) thrust coefficient and (b) power coefficient

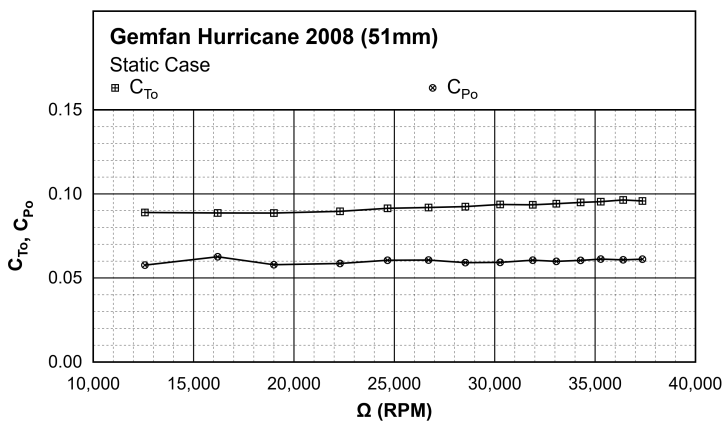

Figure 13: Combined plot of thrust coefficient and power coefficient of the left Gemfan Hurricane 2008 propeller

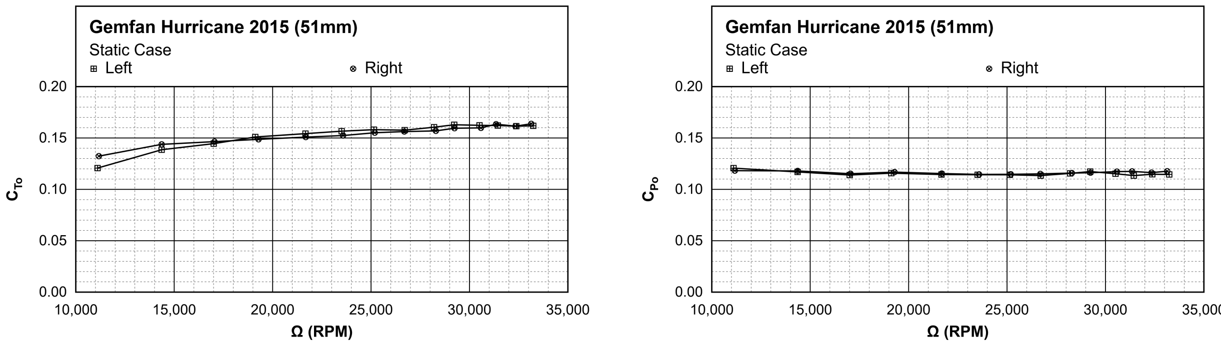

(a) (b)

Figure 14: Comparison of static performance of the left and right versions of the Gemfan Hurricane 2015 propeller: (a) thrust coefficient and (b) power coefficient

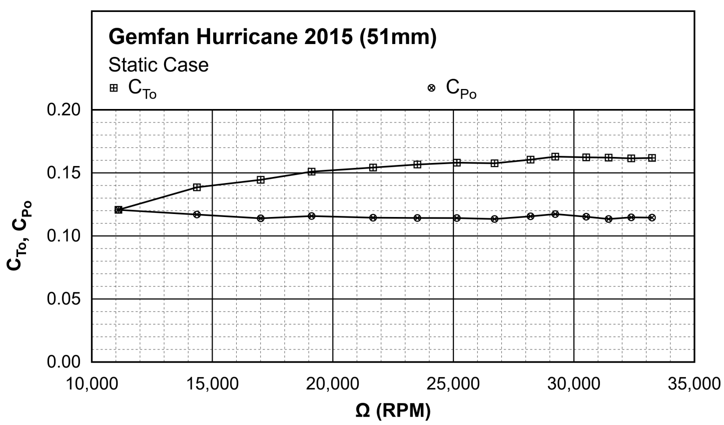

Figure 15: Combined plot of thrust coefficient and power coefficient of the left Gemfan Hurricane 2015 propeller

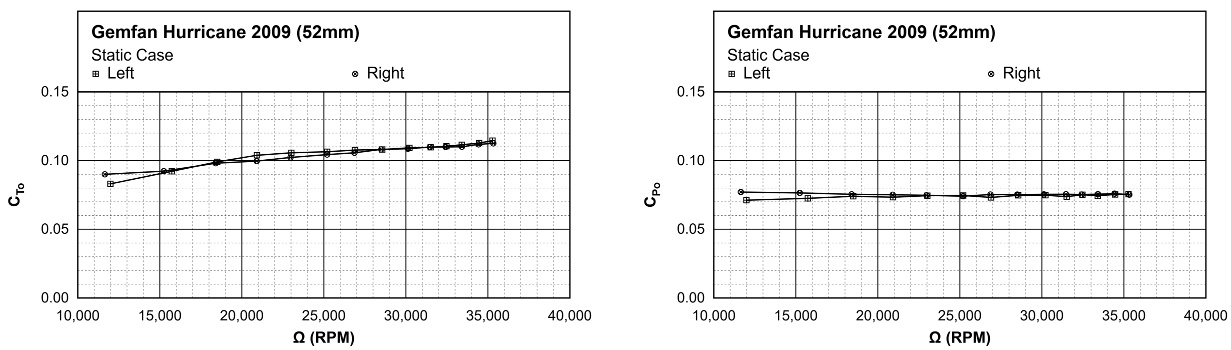

(a) (b)

Figure 16: Comparison of static performance of the left and right versions of the Gemfan Hurricane 2009 propeller: (a) thrust coefficient and (b) power coefficient

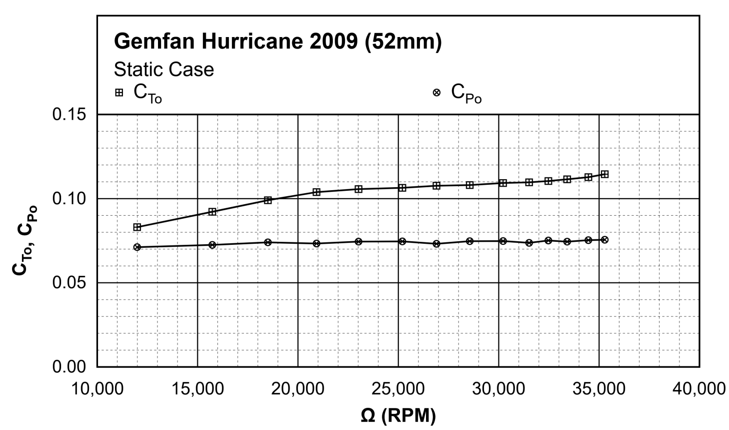

Figure 17: Combined plot of thrust coefficient and power coefficient of the left Gemfan Hurricane 2009 propeller

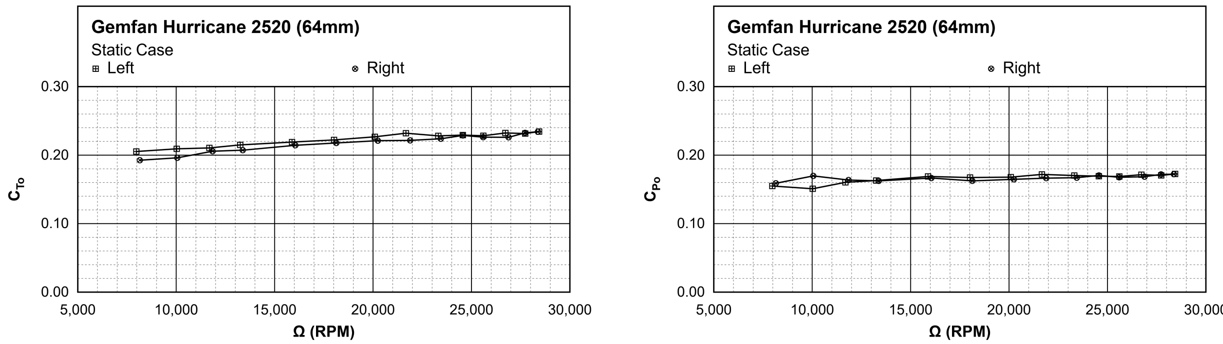

(a) (b)

Figure 18: Comparison of static performance of the left and right versions of the Gemfan Hurricane 2520 propeller: (a) thrust coefficient and (b) power coefficient

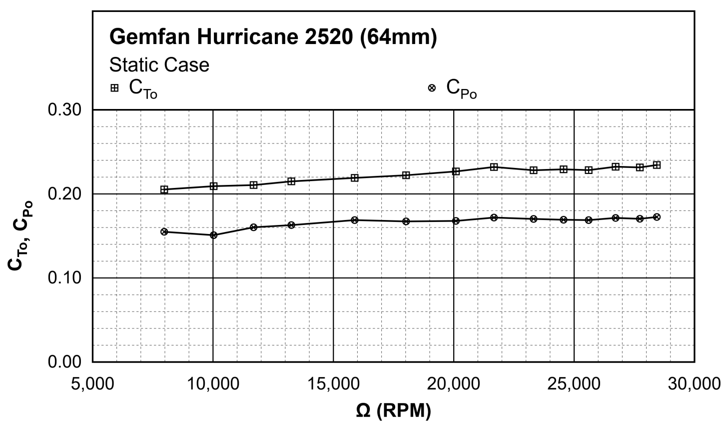

Figure 19: Combined plot of thrust coefficient and power coefficient of the left Gemfan Hurricane 2520 propeller

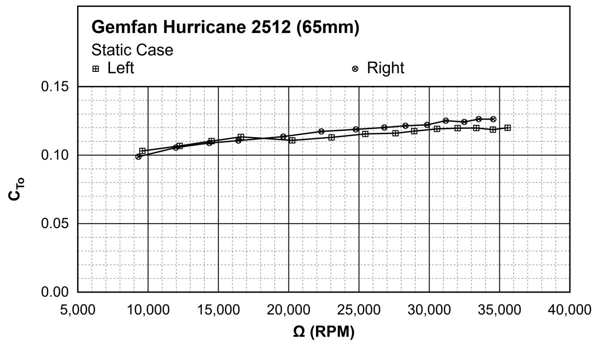

(a)

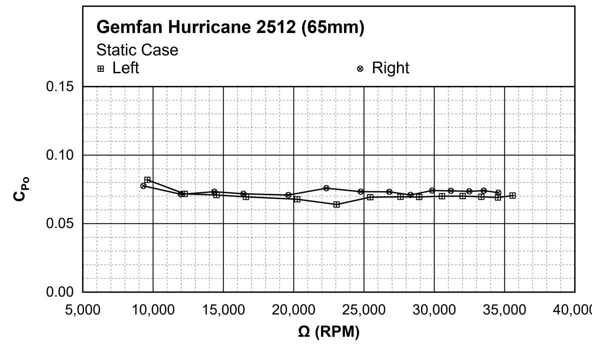

(b)

Figure 20: Comparison of static performance of the left and right versions of the Gemfan Hurricane 2512 propeller: (a) thrust coefficient and (b) power coefficient

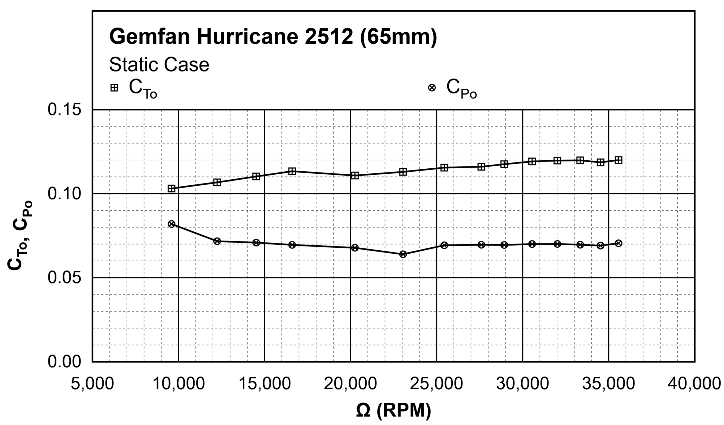

Figure 21: Combined plot of thrust coefficient and power coefficient of the left Gemfan Hurricane 2512 propeller

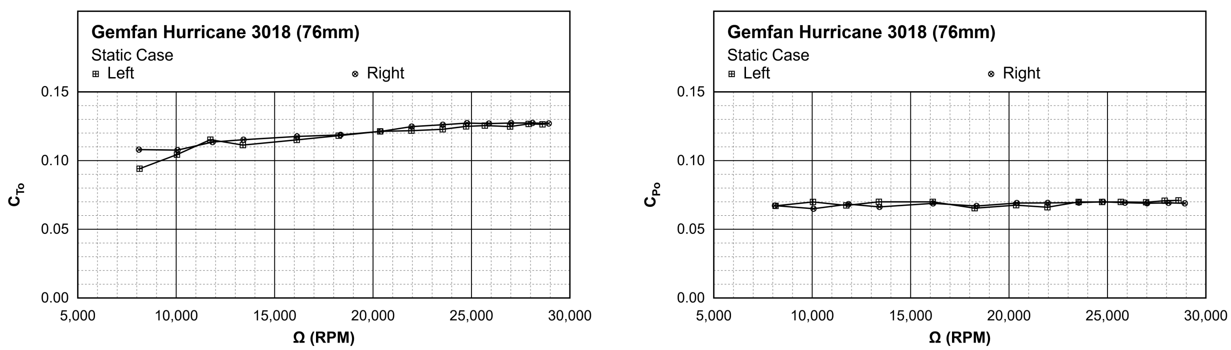

(a) (b)

Figure 22: Comparison of static performance of the left and right versions of the Gemfan Hurricane 3018 propeller: (a) thrust coefficient and (b) power coefficient

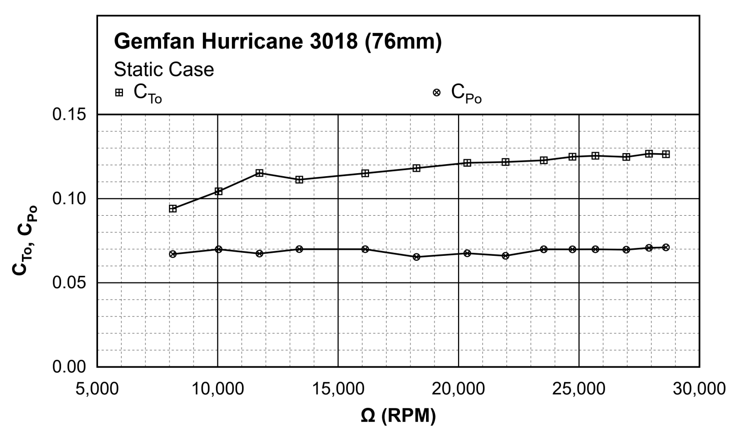

Figure 23: Combined plot of thrust coefficient and power coefficient of the left Gemfan Hurricane 3018 propeller

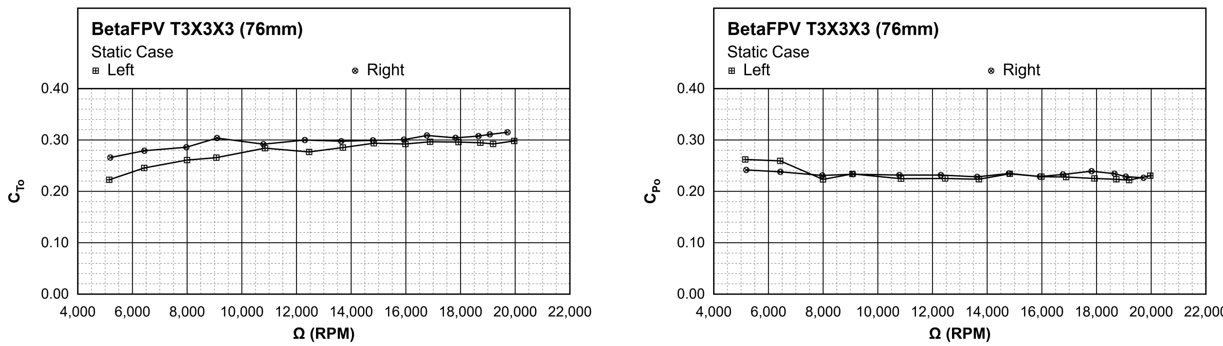

(a) (b)

Figure 24: Comparison of static performance of the left and right versions of the BetaFPV T3X3X3 propeller: (a) thrust coefficient and (b) power coefficient

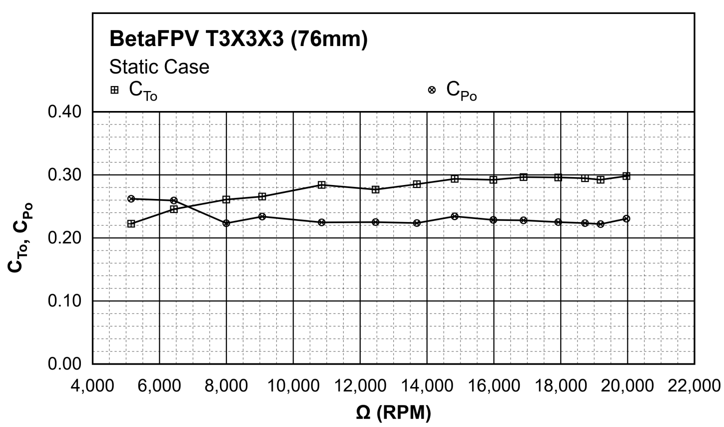

Figure 25: Combined plot of thrust coefficient and power coefficient of the left BetaFPV T3X3X3 propeller

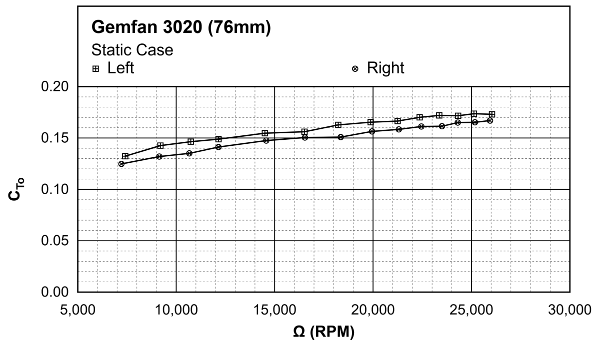

(a)

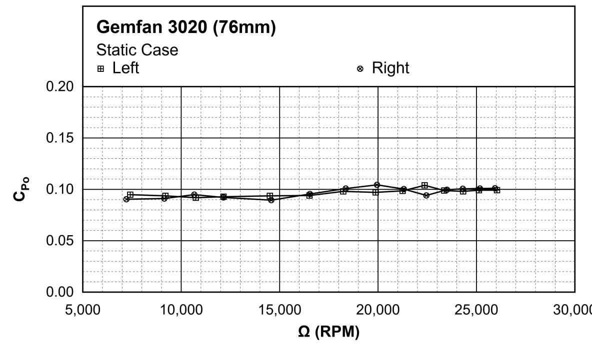

(b)

Figure 26: Comparison of static performance of the left and right versions of the Gemfan 3020 propeller: (a) thrust coefficient and (b) power coefficient

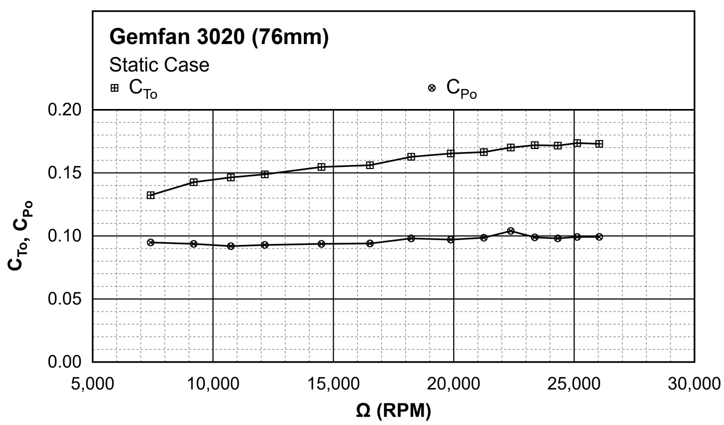

Figure 27: Combined plot of thrust coefficient and power coefficient of the left Gemfan 3020 propeller

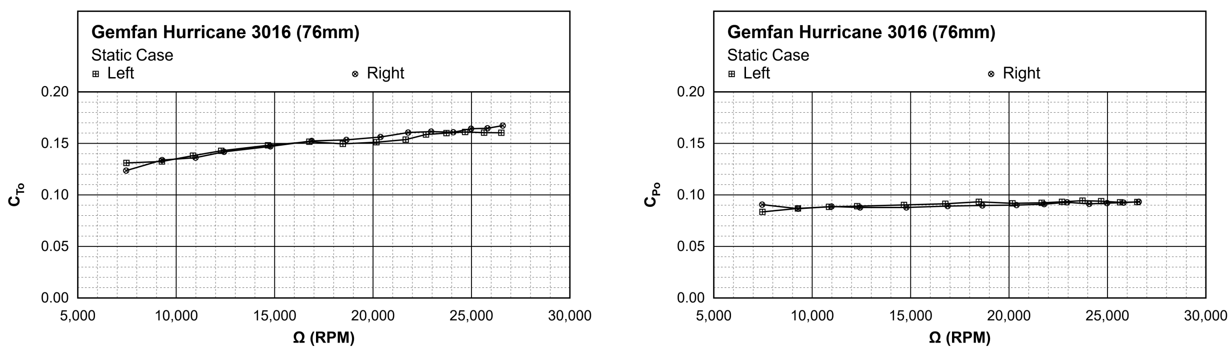

(a)

(b)

Figure 28: Comparison of static performance of the left and right versions of the Gemfan Hurricane 3016 propeller: (a) thrust coefficient and (b) power coefficient

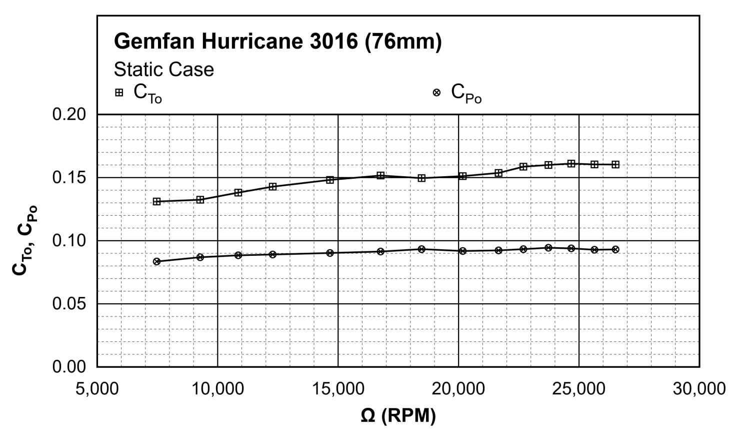

Figure 29: Combined plot of thrust coefficient and power coefficient of the left Gemfan Hurricane 3016 propeller

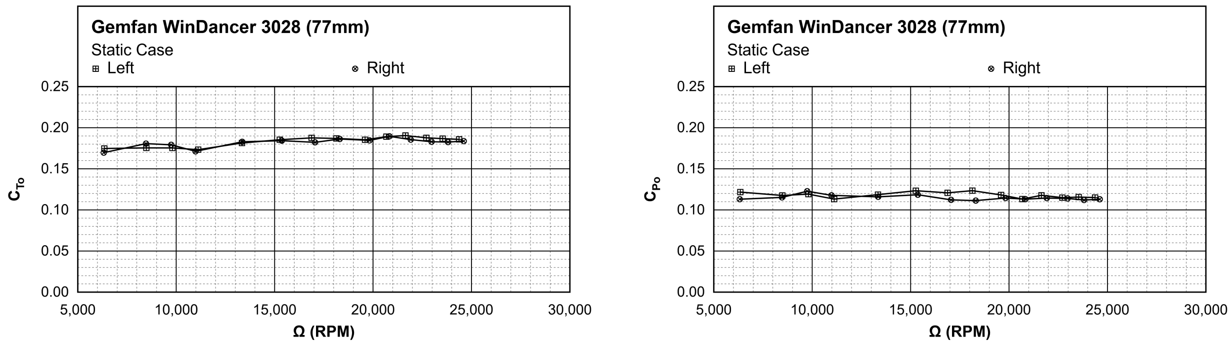

(a)

(b)

Figure 30: Comparison of static performance of the left and right versions of the Gemfan WinDancer 3028 propeller: (a) thrust coefficient and (b) power coefficient

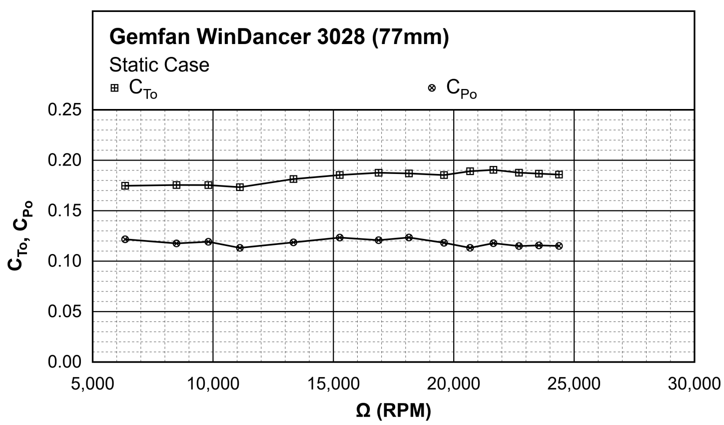

Figure 31: Combined plot of thrust coefficient and power coefficient of the left Gemfan WinDancer 3028 propeller

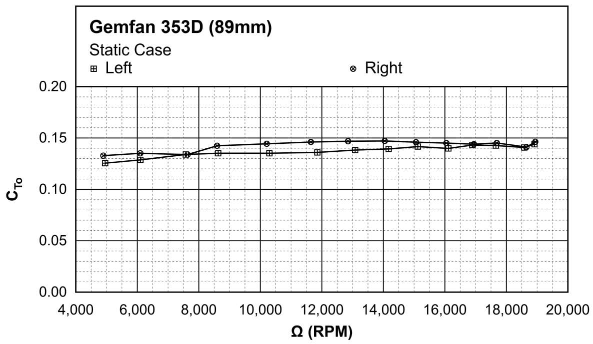

(a)

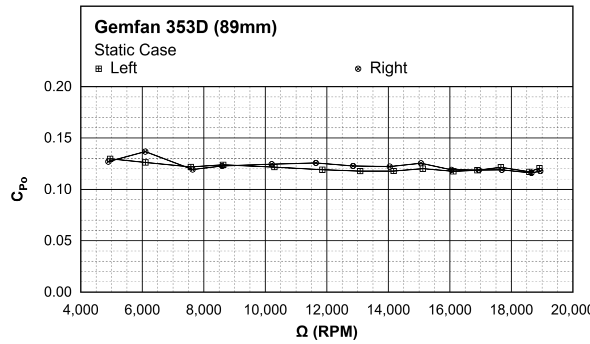

(b)

Figure 32: Comparison of static performance of the left and right versions of the Gemfan 353D propeller: (a) thrust coefficient and (b) power coefficient

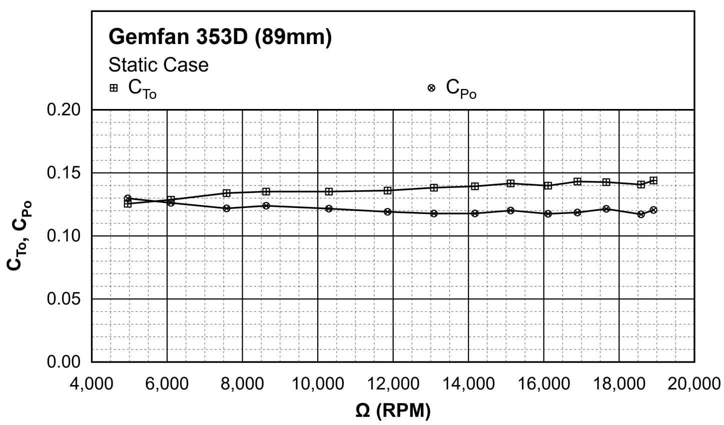

Figure 33: Combined plot of thrust coefficient and power coefficient of the left Gemfan 353D propeller

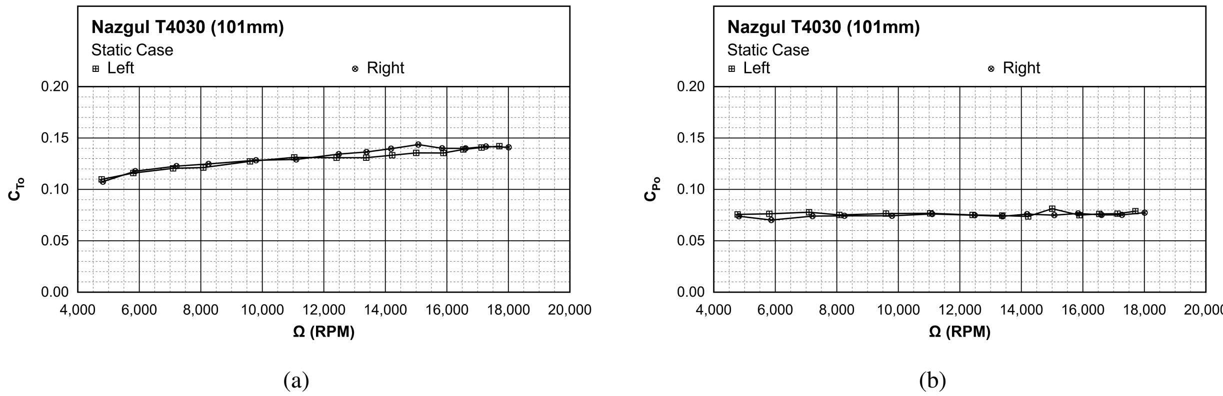

Figure 34: Comparison of static performance of the left and right versions of the Nazgul T4030 propeller: (a) thrust coefficient and (b) power coefficient

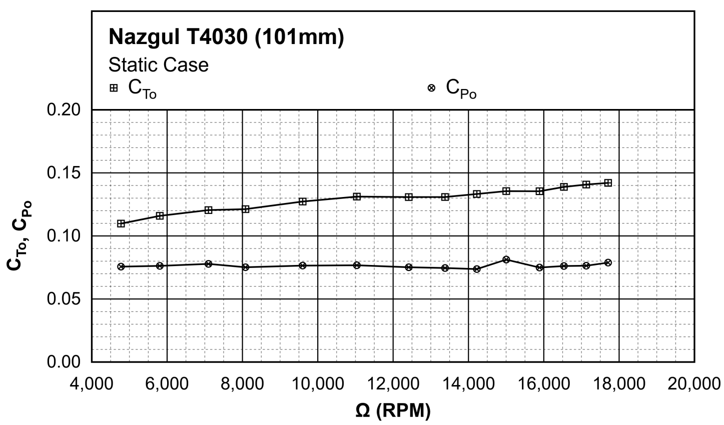

Figure 35: Combined plot of thrust coefficient and power coefficient of the left Nazgul T4030 propeller

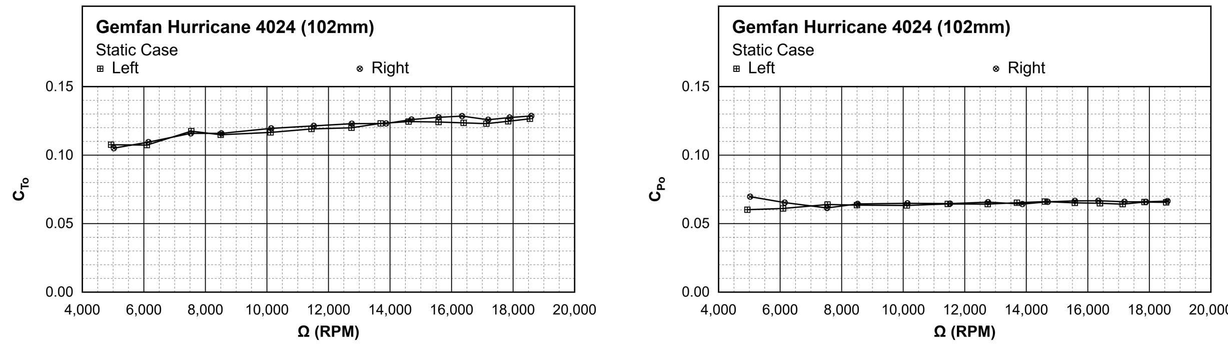

(a) (b)

Figure 36: Comparison of static performance of the left and right versions of the Gemfan Hurricane 4024 propeller: (a) thrust coefficient and (b) power coefficient

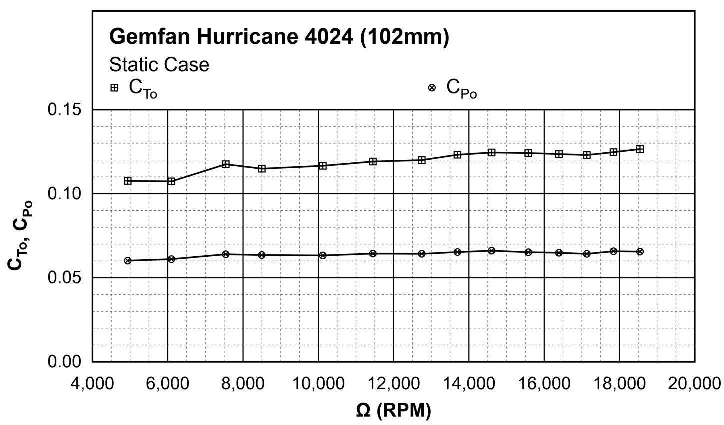

Figure 37: Combined plot of thrust coefficient and power coefficient of the left Gemfan Hurricane 4024 propeller

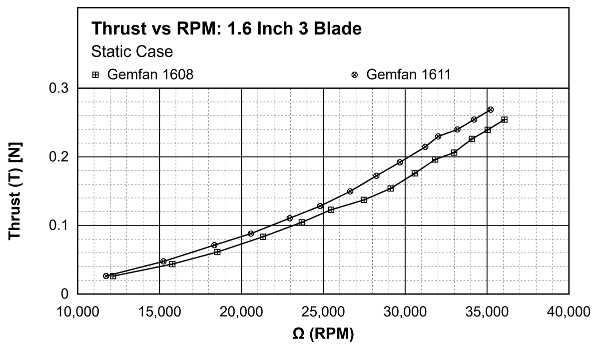

(a)

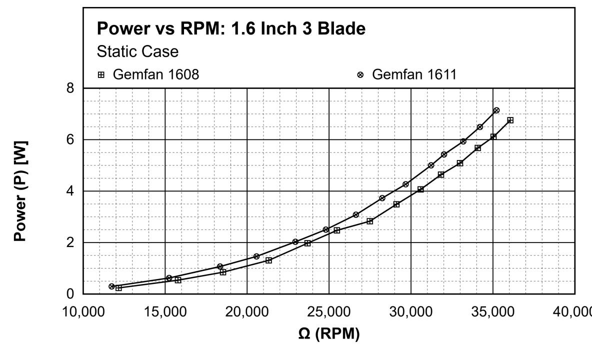

(b)

Figure 38: Comparison of 1.6 in, 3 blade propeller thrust vs PWM (a) and power vs PWM (b). The propellers compared include: Gemfan 1608, Gemfan 1611

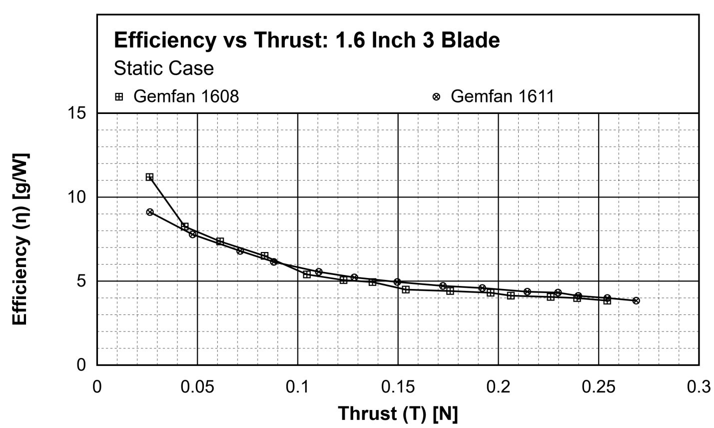

Figure 39: Comparison of 1.6 in, 3 blade propeller efficiency vs thrust. The propellers compared include: Gemfan 1608, Gemfan 1611

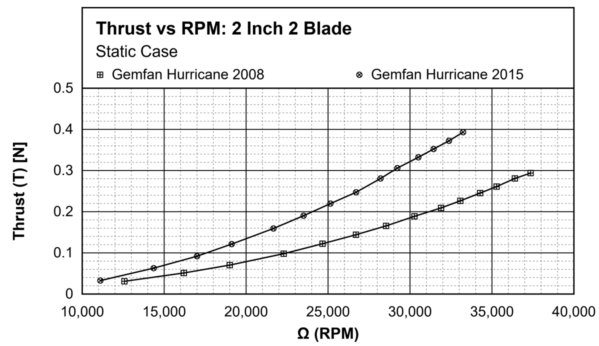

(a)

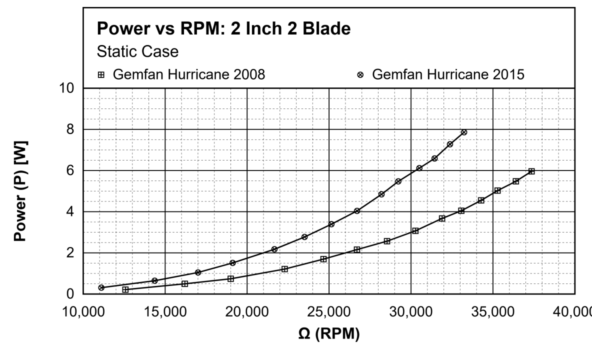

(b)

Figure 40: Comparison of 2.0 in, 2 blade propeller thrust vs PWM (a) and power vs PWM (b). The propellers compared include: Gemfan Hurricane 2008, Gemfan Hurricane 2015

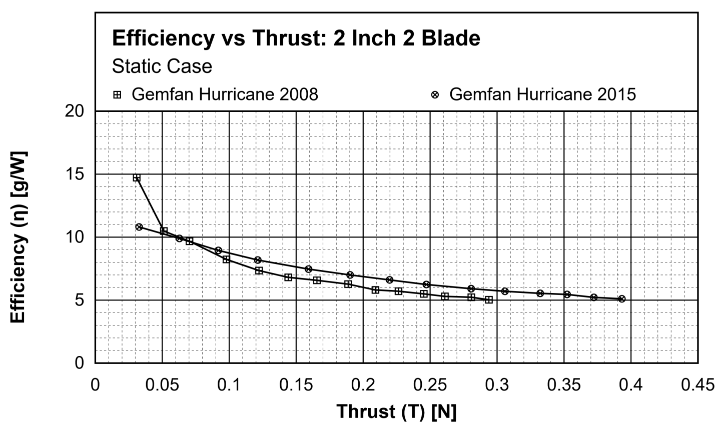

Figure 41: Comparison of 2.0 in, 2 blade propeller efficiency vs thrust. The propellers compared include: Gemfan Hurricane 2008, Gemfan Hurricane 2015

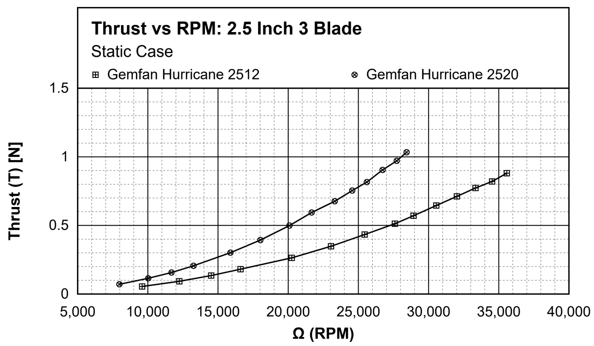

(a)

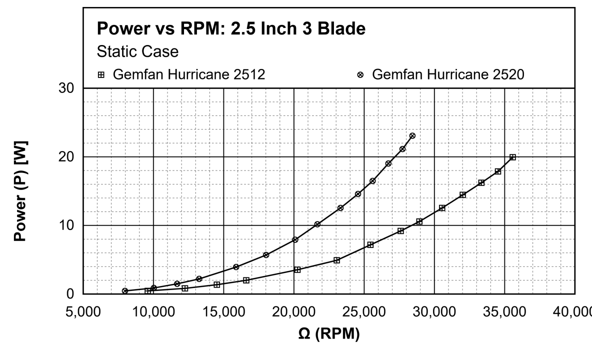

(b)

Figure 42: Comparison of 2.5 in, 3 blade propeller thrust vs PWM (a) and power vs PWM (b). The propellers compared include: Gemfan Hurricane 2520, Gemfan Hurricane 2512

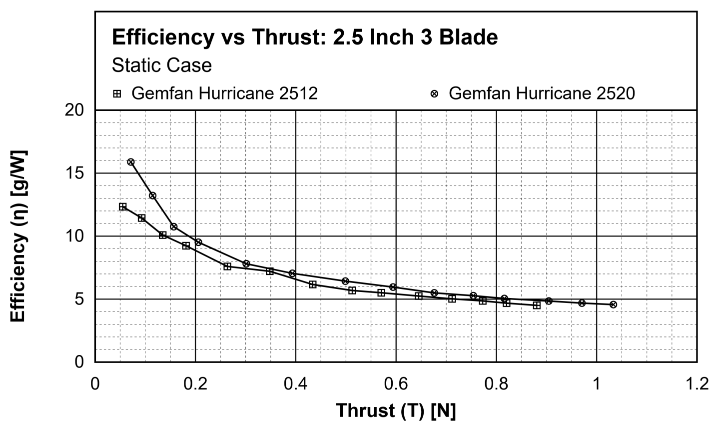

Figure 43: Comparison of 2.5 in, 3 blade propeller efficiency vs thrust. The propellers compared include: Gemfan Hurricane 2520, Gemfan Hurricane 2512

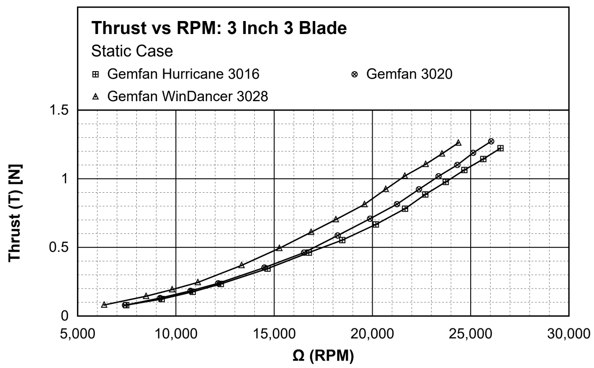

(a)

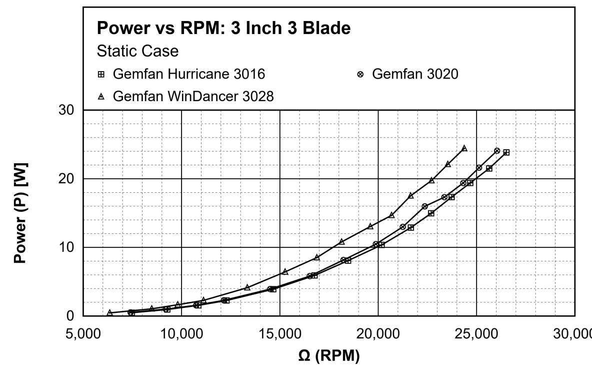

(b)

Figure 44: Comparison of 3.0 in, 3 blade propeller thrust vs PWM (a) and power vs PWM (b). The propellers compared include: Gemfan 3020, Gemfan Hurricane 3016, Gemfan WinDancer 3028

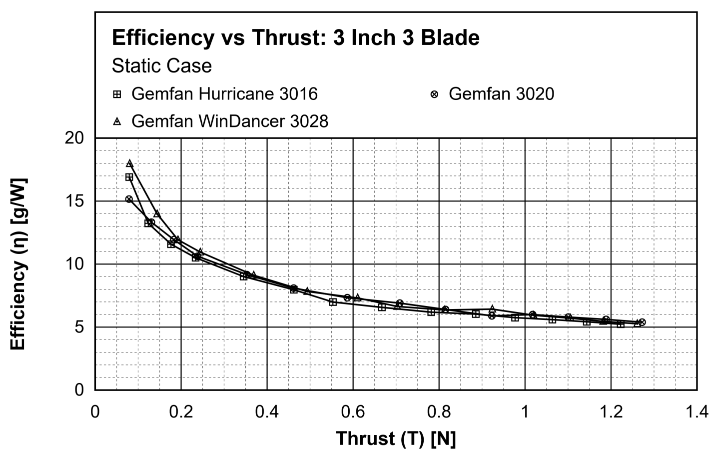

Figure 45: Comparison of 3.0 in, 3 blade propeller efficiency vs thrust. The propellers compared include: Gemfan 3020, Gemfan Hurricane 3016, Gemfan WinDancer 3028

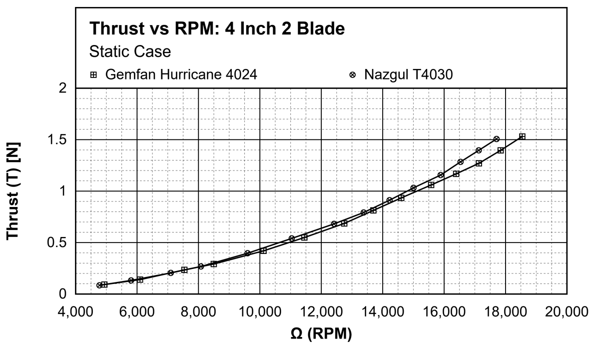

(a)

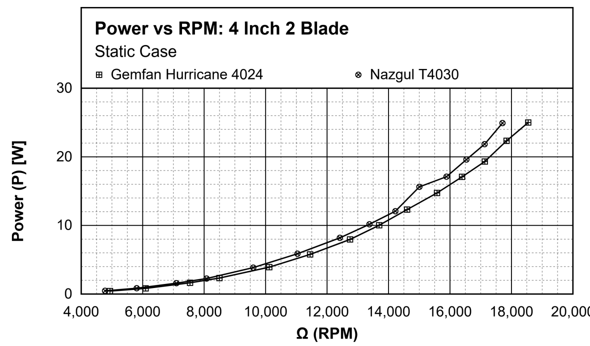

(b)

Figure 46: Comparison of 4.0 in, 2 blade propeller thrust vs PWM (a) and power vs PWM (b). The propellers compared include: Nazgul T4030, Gemfan Hurricane 4024

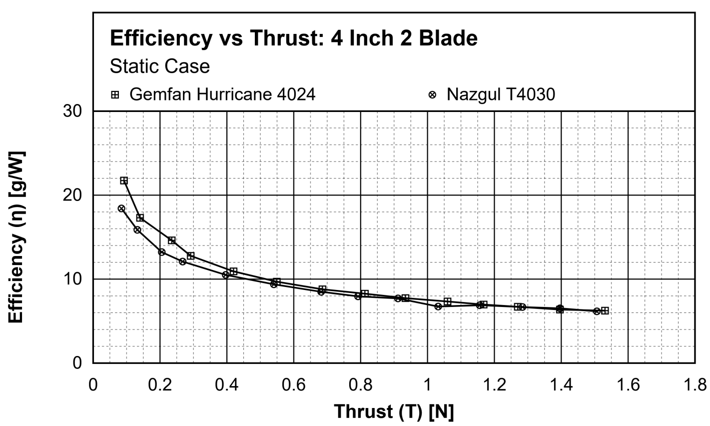

Figure 47: Comparison of 4.0 in, 2 blade propeller efficiency vs thrust. The propellers compared include: Nazgul T4030, Gemfan Hurricane 4024

IV. Summary and Future Work

This paper described the performance testing of 18 small propellers at or under 102 millimeters (4 inches) under static conditions. The motivation for profiling these propellers lies in the desire to improve the performance and efficiency of small multi-rotor and lighter-than-air vehicles, including those used in the Defend The Republic competition. The choice of propeller on these vehicles can lead to longer battery lives and faster max speeds, overall improving their usefulness. Through these tests, it was found that the left and right versions of each propeller performed very similar to each other with some minor exceptions.

Comparisons between propellers of equal diameter and blade count showed expected trends such as steeper pitch equaling higher thrust and power per RPM holding true, but no consistent correlations between propeller pitch and efficiency were found. For some size groups, the lower pitch propeller was consistently more efficient across the thrust spectrum, while other groups exhibited the opposite behavior. This observation illustrates the important fact that size and pitch alone do not determine the efficiency of a propeller, especially when it comes to propellers of very small size.

In future work, revisions will be made to the hardware and measurement procedure to improve data quality. A load cell rated for lower max force values will be substituted into the testing rig to increase the precision of lower RPM thrust measurements. Each propeller will also be tested using smaller RPM intervals to create more data-rich thrust coefficient and power coefficient curves. To increase data readability, propellers will be tested at specific RPM values as opposed to specific PWM values. More propellers will be tested in order to perform more broad and robust comparisons.

References

[1]Dantsker, O. D., Imtiaz, S., and Caccamo, M., "Electric Propulsion System Optimization for Long-Endurance and Solar-Powered Unmanned Aircraft," AIAA Paper 2019-4486, 2019 AIAA/IEEE Electric Aircraft Technologies Symposium, Indianapolis, Indiana, Aug. 2019.

[2]UIUC Applied Aerodynamics Group, "UIUC Propeller Data Site," `https://m-selig.ae.illinois.edu/props/propDB.html`.

[3]Dantsker, O. D., Caccamo, M., Deters, R. W., and Selig, M. S., "Performance Testing of Aero-Naut CAM Folding Propellers," AIAA Paper 2020-2762, AIAA Aviation Forum, Virtual Event, Jun. 2020.

[4]Dantsker, O. D., Caccamo, M., Deters, R. W., and Selig, M. S., "Performance Testing of APC Electric Fixed-Blade UAV Propellers," AIAA Paper 2022-4020, AIAA Aviation Forum, Virtual Event, Jun. 2022.

[5]Indiana University, Aerospace Systems Lab, "Defend The Republic Fall 2024," `https://www.iu-dtr.com/`.

[6]George Mason University, Patriot Pilots, "Defend The Republic Spring 2024," `https://www.sparx.vse.gmu.edu/`.

[7]Messinger, S., *Modeling, Adaptive Control, and Flight Testing of a Lighter-than-Air Vehicle Validated Using System Identification*, Master's thesis, The Pennsylvania State University, 2022, Master's Thesis.

[8]Mathew, J. P., Karri, D., Yang, J., Zhu, K., Gautam, Y., Nojima-Schmunk, K., Shishika, D., Yao, N., and Nowzari, C., "Lighter-Than-Air Autonomous Ball Capture and Scoring Robot – Design, Development, and Deployment," *arXiv preprint arXiv:2309.06352*, 2023.

[9]Mendoza, A., Lovelace, A., Potter, S., and Koziol, S., "Sensor Fusion Image Processing for Autonomous Robot Blimps," *2023 IEEE 66th International Midwest Symposium on Circuits and Systems (MWSCAS)*, 2023, pp. 312–316.

[10]Simmons, J., Lovelace, A., Tucker, D., Mendoza, A., Coates, A., Alonzo, J., Li, D., Yi, X., Potter, S., Mouritzen, I., Smith, M., Banta, C., Hodge, R., Spence, A., and Koziol, S., "Design and Construction of a Lighter than Air Robot Blimp," *2023 ASEE GSW*, No. 10.18260/1-2-1139-46327, ASEE Conferences, Denton, TX, June 2024, https://peer.asee.org/46327.

[11]Xu, J., D'antonio, D. S., Ammirato, D. J., and Saldaña, D., "SBlimp: Design, Model, and Translational Motion Control for a Swing-Blimp," *2023 IEEE/RSJ International Conference on Intelligent Robots and Systems (IROS)*, IEEE, 2023, pp. 6977–6982.

[12]Li, K., Hou, S., Negash, M., Xu, J., Jeffs, E., D'Antonio, D. S., and Saldaña, D., "A Novel Low-Cost, Recyclable, Easy-to-Build Robot Blimp For Transporting Supplies in Hard-to-Reach Locations," *2023 IEEE Global Humanitarian Technology Conference (GHTC)*, IEEE, 2023, pp. 36–42.

[13]Nojima-Schmunk, K., Turzak, D., Kim, K., Vu, A., Yang, J., Motukuri, S., Yao, N., and Shishika, D., "Manta Ray Inspired Flapping-Wing Blimp," *arXiv preprint arXiv:2310.10853*, 2023.

[14]Taylor, C. and Dantsker, O. D., "Lighter-Than-Air Vehicle Design for Target Scoring in Adversarial Conditions," AIAA Paper 2024-3896, AIAA Aviation Forum 2024, Las Vegas, NV. 2024.

[15]Dantsker, O. D., "Design, Build, and Fly Autonomous Lighter-Than-Air Vehicles as a Project-Based Class," AIAA Paper 2024-4375, AIAA Aviation Forum 2024, Las Vegas, NV. 2024.

[16]Dantsker, O. D., "Integrating Unmanned Aerial Systems into the Intelligent Systems Engineering Curriculum," Paper 2024-1185, Congress of the International Council of the Aeronautical Sciences, Florence, Italy. 2024.

[17]Taylor, C. and Dantsker, O. D., "Lighter-Than-Air-Vehicle Design for Adversarial Defense," AIAA Paper 2025-3124, AIAA Aviation Forum 2025, Las Vegas, NV. 2025.

[18]Taylor, C., Widjaja, M., and Dantsker, O. D., "Remotely-Processed Vision-Based Control of Autonomous Lighter-Than-Air UAVs With Real-Time Constraints," AIAA Paper 2025-1344, AIAA SciTech Forum 2025, Orlando, FL. 2025.

[19]Widjaja, M., Taylor, C., and Dantsker, O. D., "Viability of NPU-Equipped SBCs for Real-Time Onboard Vision Autonomy on Lighter-Than-Air UAVs," AIAA Paper 2025-3546, AIAA Aviation Forum 2025, Las Vegas, NV. 2025.

[20]Brandt, J. B., *Small-Scale Propeller Performance at Low Speeds*, Master's thesis, University of Illinois at Urbana-Champaign, Department of Aerospace Engineering, Urbana, IL, 2005.

[21]Brandt, J. B. and Selig, M. S., "Propeller Performance Data at Low Reynolds Numbers," AIAA Paper 2011-1255, AIAA Aerospace Sciences Meeting, Orlando, Florida, Jan. 2011.

[22]Uhlig, D. V., *Post Stall Propeller Behavior at Low Reynolds Numbers*, Master's thesis, University of Illinois at Urbana-Champaign, Department of Aerospace Engineering, Urbana, IL, 2007.

[23]Uhlig, D. V. and Selig, M. S., "Post Stall Propeller Behavior at Low Reynolds Numbers," AIAA Paper 2008-407, AIAA Aerospace Sciences Meeting, Reno, Nevada, Jan. 2008.

[24]Lundstrom, D., *Aircraft Design Automation and Subscale Testing*, Ph.D. thesis, Linkoping University, Department of Management and Engineering, Linkoping, Sweden, 2012.

[25]Lundstrom, D. and Krus, P., "Testing of Atmospheric Turbulence Effects on the Performance of Micro Air Vehicles," *International Journal of Micro Air Vehicles*, Vol. 4, No. 2, Jun. 2012, pp. 133–149.

[26]Deters, R. W. and Selig, M. S., "Static Testing of Micro Propellers," AIAA Paper 2008-6246, AIAA Applied Aerodynamics InProceedings, Honolulu, Hawaii, Aug. 2008.

[27]Deters, R. W., *Performance and Slipstream Characteristics of Small-Scale Propelllers at Low Reynolds Numbers*, Ph.D. thesis, University of Illinois at Urbana-Champaign, Department of Aerospace Engineering, Urbana, IL, 2014.

[28]Deters, R. W., Kleinke, S., and Selig, M. S., "Static Testing of Propulsion Elements for Small Multirotor Unmanned Aerial Vehicles," AIAA Paper 2017-3743, AIAA Aviation Forum, Denver, Colorado, June 2017.

[29]Deters, R. W., Dantsker, O. D., Kleinke, S., Norman, N., and Selig, M. S., "Static Performance Results of Propellers Used on Nano, Micro, and Mini Quadrotors," AIAA Paper 2018-4122, AIAA Aviation Forum, Atlanta, Georgia, June 2018.

[30]Lindahl, P., Moog, E., and Shaw, S. R., "Simulation, Design, and Validation of an UAV SOFC Propulsion System," *IEEE Transactions on Aerospace and Electronic Systems*, Vol. 48, No. 3, Jul. 2012, pp. 2582–2593.

[31]Chaney, C. S., Bahrami, J. K., Gavin, P. A., Shoemake, E. D., Barrow, E. S., and Matveev, K. I., "Car-Top Test Module as a Low-Cost Alternative to Wind Tunnel Testing of UAV Propulsion Systems," *Journal of Aerospace Engineering*, Vol. 27, No. 6, Nov. 2014.

[32]Dantsker, O. D., Selig, M. S., and Mancuso, R., " A Rolling Rig for Propeller Performance Testing," AIAA Paper 2017-3745, AIAA Applied Aerodynamics InProceedings, Denver, Colorado, June 2017.

[33]Drela, M., "DC Motor / Propeller Matching," `http://web.mit.edu/drela/Public/web/qprop/motorprop.pdf`.

[34]Drela, M., "First-Order DC Electric Motor Model," `http://web.mit.edu/drela/Public/web/qprop/motor1\_theory.pdf`.

[35]Drela, M., "Second-Order DC Electric Motor Model," `http://web.mit.edu/drela/Public/web/qprop/motor2\_theory.pdf`.

[36]Green, C. R. and McDonald, R. A., "Modeling and Test of the Eciency of Electronic Speed Controllers for Brushless DC Motors," AIAA Paper 2015-3191, AIAA Aviation Forum, Dallas, Texas, Jun. 2015.

[37]Gong, A. and Verstraete, D., "Experimental Testing of Electronic Speed Controllers for UAVs," AIAA Paper 2017-4955, AIAA/SAE/ASEE Joint Propulsion InProceedings, Atlanta, Georgia, July 2017.

[38]Gong, A., MacNeill, R., and Verstraete, D., "Performance Testing and Modeling of a Brushless DC Motor, Electronic Speed Controller and Propeller for a Small UAV," AIAA Paper 2018-4584, AIAA Propulsion and Energy Forum, Cincinnati, Ohio, July 2018.

[39]Gong, A., Maunder, H., and Verstraete, D., "Development of an in-fight thrust measurement system for UAVs," AIAA Paper 2017-5092, AIAA/SAE/ASEE Joint Propulsion InProceedings, Atlanta, Georgia, July 2017.

[40]Cox, B., Dantsker, O. D., and Deters, R. W., "Propulsion System Testing Instrumentation for Multi-Rotor and Lighter-Than-Air UAVs," AIAA Paper, 2025-0252, AIAA SciTech Forum 2025, Orlando, FL. 2025.